

# Marine incursion into South America

The Amazon basin harbours the most diverse assemblage of freshwater fishes in the world, including a disproportionately large number of marine-derived groups, such as stingrays, flatfishes, pufferfishes, and anchovies<sup>1</sup>. On the basis of our molecular phylogenetic analysis of South American freshwater stingrays (Potamotrygonidae), coupled with reconstructions of Amazonian palaeogeography, we propose that some marine-derived freshwater fish species originated as a by-product of massive movements of marine waters into the upper Amazon region during the Early Miocene epoch, 15–23 million years ago.

Miocene South America experienced profound changes of topography, environment and river drainage patterns<sup>2,3</sup>. A combination of sea-level changes and tectonic loading of the foreland basin in the upper Amazon produced significant incursions of sea water, as indicated by the presence of marine and brackish mollusc, copepod and mangrove fossils<sup>4,5</sup>. Nuttall<sup>4</sup> says the upper Amazon during the Miocene was “up to 500 km wide, occupied by a continually shifting pattern of streams, swamps, and lakes of varying salinity and offering intermittent connections with the Caribbean”. These conditions would have been ideal for the isolation of marine fishes in progressively desalinated habitats. We suggest, therefore: first, that the divergence between potamotrygonid stingrays and their closest marine relative should have occurred during the Miocene; and second, that the distribution of the closest marine relative should include the Caribbean, a proposed source of the marine incursion.

To test the marine-incursion hypothesis, we investigated the evolutionary history of stingrays using DNA sequences from the gene encoding mitochondrial cytochrome *b* (Fig. 1a). We analysed sequences from ten South American freshwater stingrays, including representatives of all three potamotrygonid genera, and from all the supposed marine relatives of potamotrygonids. We calibrated a rate for cytochrome *b* evolution in potamotrygonids based on the amount of sequence divergence between species separated by a known geological event, the uplift of both the eastern cordillera of the Andes and the Merida Andes, which isolated the Maracaibo stingray (*Potamotrygon yepezi*) approximately 8 million years ago<sup>2,3</sup>.

Based on our cytochrome *b* calibration and phylogenetic tree, the estimated divergence time between potamotrygonids and their closest marine relative indicates that neotropical freshwater stingrays originated in the Early Miocene. Moreover, one of the two species that are the marine relatives of

the freshwater rays is distributed along the northern coast of South America (Fig. 1b). Both the estimated origination time of the freshwater species and the biogeography of the closest marine relative are therefore consistent with predictions of the marine-incursion hypothesis.

Alternative explanations have been advanced to account for the presence of marine-derived taxa in South America. For instance, it has been suggested<sup>1</sup> that the extensive interface between marine and freshwater habitats in the lower Amazon served as a gateway for marine invaders of neotropical rivers. Such invasion hypotheses are difficult to refute because they are compatible with many different biogeographical patterns. Invasions are essentially opportunistic, and we might expect fresh water to have been colonized several times; however,

even though South American rivers have been open to the oceans for more than 100 million years, endemic freshwater stingrays have a single, unique origin. We believe that this pattern argues against invasions by marine rays, and suggests instead that a single geological event, such as a marine incursion, was crucial.

It has also been proposed that uplift of the Andes blocked a previously westward-draining proto-Amazon, and isolated a component of the Pacific marine fauna in progressively desalinated inland lakes or seas. This would mean a Late Cretaceous or Palaeocene origin for Potamotrygonidae, as this is when Andean uplift probably severed the last connection between the Pacific Ocean and the upper Amazon<sup>9</sup>. But we estimate that potamotrygonids originated more recently, and the marine relative of

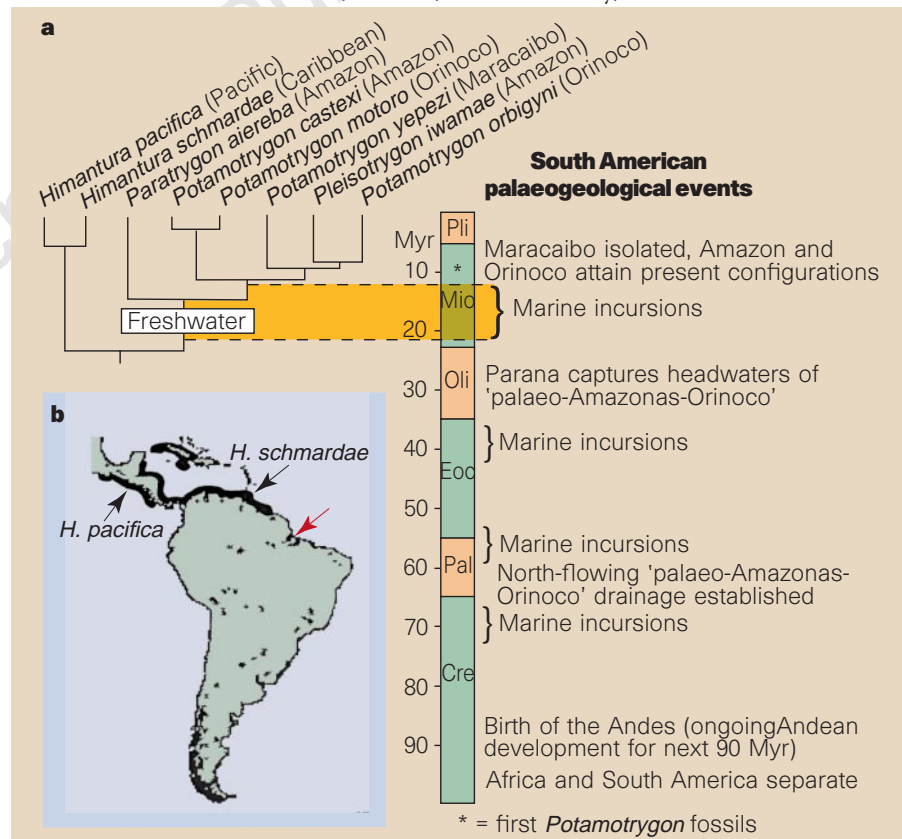


**Figure 1** Phylogeny and biogeography of freshwater stingrays. **a**, Phylogenetic hypothesis for freshwater stingrays and their closest marine relative, and timescale showing palaeogeological events in South America<sup>2,3</sup>. Relationships of Potamotrygonidae, ampho-American *Himantura* and seven other stingray genera were inferred from parsimony analysis of 765 base pairs of cytochrome *b* sequence, with transitions at third codon positions weighted one-fifth of all other changes<sup>10</sup> (not all taxa shown; sequences available from Genbank). The potamotrygonid species are a monophyletic group, so neotropical freshwater rays had a single origin. *H. pacifica* and *H. schmardae* were supported as the closest sister taxa to potamotrygonids, consistent with morphological analysis<sup>9</sup>. Ages of nodes were estimated from transversion distances at third positions to minimize effects of saturation and selection. The estimated age of *Potamotrygon* agrees with putative fossil evidence for this taxon<sup>12</sup>. **b**, Distribution of *H. pacifica* and *H. schmardae* (black areas along coastlines), the closest marine relatives of the freshwater rays. The group is found in the Caribbean (the proposed source of Miocene marine incursions) but not the mouth of the Amazon (red arrow) or along the Pacific coast of South America (other proposed points of colonization).

freshwater stingrays does not occur along the Pacific coast of South America (Fig. 1b).

A diverse cross-section of the South American river fauna, including dolphins, fishes, crabs and snails, appear to be derived from marine ancestors. If these taxa originated contemporaneously with freshwater stingrays, the Miocene marine transgressions of South America will have had a profound effect on the diversification and structuring of neotropical communities.

Nathan R. Lovejoy\*,

Eldredge Bermingham†, Andrew P. Martin‡

\*Section of Ecology and Systematics,

Corson Hall, Cornell University,

Ithaca, New York 14853-2701, USA

†Smithsonian Tropical Research Institute,

Naos Marine Laboratory,

PO Box 2072, Balboa, Republic of Panama

‡Department of EPOB, CB 334,

University of Colorado,

Boulder, Colorado 80309, USA

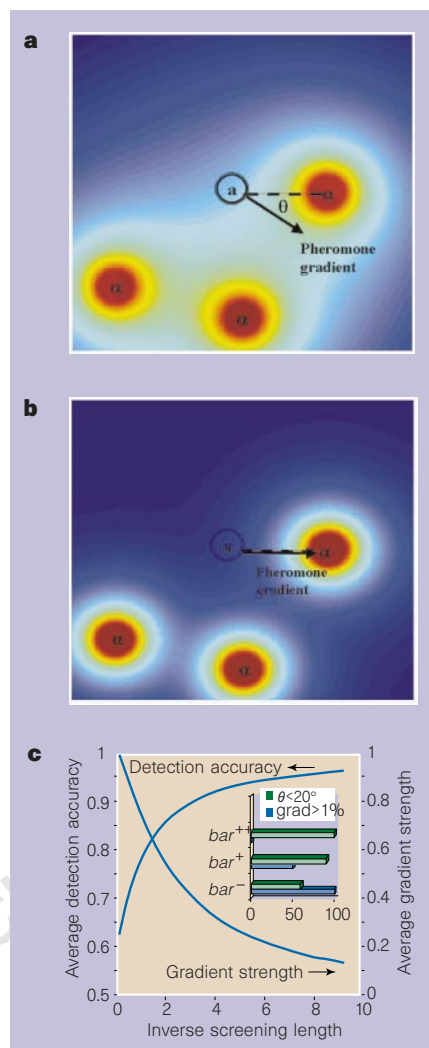
e-mail: am@stripe.colorado.edu

1. Roberts, T. R. *Bull. Mus. Comp. Zool.* **143**, 117–147 (1972).
2. Hoorn, C. *et al. Geology* **23**, 237–240 (1995).
3. Lundberg, J. G. *et al. in Phylogeny and Classification of Neotropical Fishes* (eds Malabarba, L. R., Reis, R. E., Vari, R. P., Lucena, C. A. S. & Lucena, Z. M. S.) (Museu de Ciências e Tecnologia, Porto Alegre, Brazil, in the press).
4. Nuttall, C. P. *Bull. Br. Mus. Nat. Hist.* **45**, 165–371 (1990).
5. Hoorn, C. *Palaeogeogr. Palaeoclimatol. Palaeoecol.* **105**, 267–309 (1993).
6. Croizat, L. *Space, Time, Form: The Biological Synthesis* (Published by the author, Caracas, Venezuela, 1962).
7. Brooks, D. R., Thorson, T. B. & Mayes, M. A. in *Advances in Cladistics* (eds Funk, V. A. & Brooks, D. R.) 147–175 (New York Botanical Garden, 1981).
8. Grabert, H. *Natur Mus.* **113**, 61–71 (1983).
9. Kroonenberg, S. B., Bakker, J. G. M. & van der Wiel, A. M. *Geol. Mijnb.* **69**, 279–290 (1990).
10. Swofford, D. L. *PAUP: Phylogenetic Analysis Using Parsimony, version 3.1* (Illinois Natural History Survey, Champaign, 1993).
11. Lovejoy, N. R. *Zool. J. Linn. Soc.* **117**, 207–257 (1996).
12. Lundberg, J. G. in *Phylogeny and Classification of Neotropical Fishes* (eds Malabarba, L. R., Reis, R. E., Vari, R. P., Lucena, C. A. S. & Lucena, Z. M. S.) (Museu de Ciências e Tecnologia, Porto Alegre, Brazil, in the press).

## Protease helps yeast find mating partners

The choice of mating partner by the yeast *Saccharomyces cerevisiae* involves the detection of mating pheromones produced by other yeast cells. A cell that is capable of mating deduces the position of its nearest mating partner from the spatial gradient of pheromone. While studying this process, we realized that, in the presence of many potential mating partners, the gradient might not point in the direction of the nearest partner. Here we show that degradation of some of the mating pheromone by protease enzymes helps to align the gradient in the direction of the nearest partner, which increases mating efficiency.

Haploid yeast cells of the two mating types, a and α, signal to each other by the secretion of cell-type-specific pheromones



(a-factor and α-factor, respectively), which are detected by cells of the opposite mating type, triggering a series of events that lead to mating. In particular, the cell response includes directed growth towards the mating partner, the position of which is estimated from the direction of maximum pheromone concentration<sup>1–3</sup>. Because yeast cells do not move, an appropriate choice of growth direction is essential for efficient mating.

Cells of mating type a secrete a protease that hydrolyses α-factor<sup>4,5</sup>. Mutants deficient in this ‘barrier activity’ (*bar1* mutants<sup>6,7</sup>) are highly sensitive to pheromones<sup>7</sup>, so the protease was thought to be involved in the recovery of yeast cells from the pheromone-induced cell-cycle arrest that is part of the pre-mating response. But *bar1* mutants also mate less efficiently with α-cells in a mass mating mixture<sup>1</sup>. A role for the protease in mating-partner detection has also been suggested<sup>4</sup>.

To understand how the protease may increase mating efficiency, consider an a-cell surrounded by several α-cells, which secrete α-factor (Fig. 1a,b). These cells are part of a larger population of a- and α-cells. The steady-state profile of pheromone concentration between cells,  $[P(\mathbf{r})]$ , where  $\mathbf{r}$

represents a position in three-dimensional space, is given by solving the diffusion equation  $\partial[P(\mathbf{r})]/\partial t = D\nabla^2[P(\mathbf{r})] = 0$ , where  $D$  is the diffusion coefficient. It is useful to consider an analogy with an electrostatic system, as the electrostatic potential satisfies the above equation. The α-cells can be thought of as electrostatic point charges, the pheromone concentration as an electrostatic potential, and the pheromone gradient as an electric field. The pheromone profile is given by:  $[P(\mathbf{r})] = \sum_{i=1}^N \phi(\mathbf{r} - \mathbf{r}_i)$ ,  $\phi(|\mathbf{r}|) = 1/|\mathbf{r}|$  where  $\phi(\mathbf{r} - \mathbf{r}_i)$  is the contribution of the  $i$ th cell, located at  $\mathbf{r}_i$ , to the concentration. Because  $1/r$  is a slowly decaying function of the radial distance,  $r$ , the pheromone concentration at any point is determined by the contribution of many α-cells. In general, therefore, the pheromone gradient at the location of an a-cell will not point in the direction of the nearest mating partner, but at an angle,  $\theta$ , from it (Fig. 1a). But what is the role of the protease? Consider first-order degradation:  $\partial[P(\mathbf{r})]/\partial t = D\nabla^2[P(\mathbf{r})] - k[B][P(\mathbf{r})] = 0$  where  $[B]$  is the concentration of the *bar* protease, and  $k$  is a kinetic rate constant. In terms of the electrostatic analogy, the new

Figure 1 Protease secretion improves detection of the nearest mating partner. a,b, An a-cell is surrounded by α-cells, which secrete α-factor mating pheromones. The steady-state pheromone concentration ranges from high (red) to low (dark blue). The a-cell grows up the pheromone gradient. a, In the absence of protease, the pheromone gradient is determined by many α-cells, leading to a failure to locate the nearest mating partner: the angle between the direction to the nearest mating cell and the direction of the pheromone gradient (and thus the direction of growth),  $\theta$ , is not zero. b, Widely diffused protease hydrolyses the α-factor, limiting the range of pheromone diffusion and improving the detection of the nearest mating partner. c, Average detection accuracy  $\langle \cos \theta \rangle$ , and the average magnitude of the pheromone gradient,  $\langle |\nabla[P]| \rangle$ , as functions of the inverse screening length,  $1/\lambda$ . We placed 10,000 cells randomly in a three-dimensional cube and calculated the pheromone gradient at the centre. The screening length,  $\lambda$ , was normalized by the mean distance between cells; the average strength of the gradient was normalized by its maximum (obtained for zero screening, with  $\lambda = \infty$ );  $\theta$  is the angle between the direction of the gradient and the direction to the cell nearest the centre. Detection accuracy increases rapidly for  $\lambda \approx 1$ . Minimum accuracy occurs at  $\lambda = \infty$ , which corresponds to an error of  $\theta = 50^\circ$ . Inset, effect of the *bar* protease on the detection of the nearest mating partner. Blue columns show percentage of cells exposed to a pheromone gradient with normalized values of more than 1%. Green columns show the probability that this gradient will point to within  $20^\circ$  of the nearest α-cell. Strain names are arbitrary: *bar-* indicates cells that do not secrete protease; *bar+*, protease-secreting cells with  $1/\lambda = 4$ ; and *bar++*, cells that secrete a higher level of protease, with  $1/\lambda = 10$ .

Figure 1 Protease secretion improves detection of the nearest mating partner. a,b, An a-cell is surrounded by α-cells, which secrete α-factor mating pheromones. The steady-state pheromone concentration ranges from high (red) to low (dark blue). The a-cell grows up the pheromone gradient. a, In the absence of protease, the pheromone gradient is determined by many α-cells, leading to a failure to locate the nearest mating partner: the angle between the direction to the nearest mating cell and the direction of the pheromone gradient (and thus the direction of growth),  $\theta$ , is not zero. b, Widely diffused protease hydrolyses the α-factor, limiting the range of pheromone diffusion and improving the detection of the nearest mating partner. c, Average detection accuracy  $\langle \cos \theta \rangle$ , and the average magnitude of the pheromone gradient,  $\langle |\nabla[P]| \rangle$ , as functions of the inverse screening length,  $1/\lambda$ . We placed 10,000 cells randomly in a three-dimensional cube and calculated the pheromone gradient at the centre. The screening length,  $\lambda$ , was normalized by the mean distance between cells; the average strength of the gradient was normalized by its maximum (obtained for zero screening, with  $\lambda = \infty$ );  $\theta$  is the angle between the direction of the gradient and the direction to the cell nearest the centre. Detection accuracy increases rapidly for  $\lambda \approx 1$ . Minimum accuracy occurs at  $\lambda = \infty$ , which corresponds to an error of  $\theta = 50^\circ$ . Inset, effect of the *bar* protease on the detection of the nearest mating partner. Blue columns show percentage of cells exposed to a pheromone gradient with normalized values of more than 1%. Green columns show the probability that this gradient will point to within  $20^\circ$  of the nearest α-cell. Strain names are arbitrary: *bar-* indicates cells that do not secrete protease; *bar+*, protease-secreting cells with  $1/\lambda = 4$ ; and *bar++*, cells that secrete a higher level of protease, with  $1/\lambda = 10$ .

Figure 1 Protease secretion improves detection of the nearest mating partner. a,b, An a-cell is surrounded by α-cells, which secrete α-factor mating pheromones. The steady-state pheromone concentration ranges from high (red) to low (dark blue). The a-cell grows up the pheromone gradient. a, In the absence of protease, the pheromone gradient is determined by many α-cells, leading to a failure to locate the nearest mating partner: the angle between the direction to the nearest mating cell and the direction of the pheromone gradient (and thus the direction of growth),  $\theta$ , is not zero. b, Widely diffused protease hydrolyses the α-factor, limiting the range of pheromone diffusion and improving the detection of the nearest mating partner. c, Average detection accuracy  $\langle \cos \theta \rangle$ , and the average magnitude of the pheromone gradient,  $\langle |\nabla[P]| \rangle$ , as functions of the inverse screening length,  $1/\lambda$ . We placed 10,000 cells randomly in a three-dimensional cube and calculated the pheromone gradient at the centre. The screening length,  $\lambda$ , was normalized by the mean distance between cells; the average strength of the gradient was normalized by its maximum (obtained for zero screening, with  $\lambda = \infty$ );  $\theta$  is the angle between the direction of the gradient and the direction to the cell nearest the centre. Detection accuracy increases rapidly for  $\lambda \approx 1$ . Minimum accuracy occurs at  $\lambda = \infty$ , which corresponds to an error of  $\theta = 50^\circ$ . Inset, effect of the *bar* protease on the detection of the nearest mating partner. Blue columns show percentage of cells exposed to a pheromone gradient with normalized values of more than 1%. Green columns show the probability that this gradient will point to within  $20^\circ$  of the nearest α-cell. Strain names are arbitrary: *bar-* indicates cells that do not secrete protease; *bar+*, protease-secreting cells with  $1/\lambda = 4$ ; and *bar++*, cells that secrete a higher level of protease, with  $1/\lambda = 10$ .

Figure 1 Protease secretion improves detection of the nearest mating partner. a,b, An a-cell is surrounded by α-cells, which secrete α-factor mating pheromones. The steady-state pheromone concentration ranges from high (red) to low (dark blue). The a-cell grows up the pheromone gradient. a, In the absence of protease, the pheromone gradient is determined by many α-cells, leading to a failure to locate the nearest mating partner: the angle between the direction to the nearest mating cell and the direction of the pheromone gradient (and thus the direction of growth),  $\theta$ , is not zero. b, Widely diffused protease hydrolyses the α-factor, limiting the range of pheromone diffusion and improving the detection of the nearest mating partner. c, Average detection accuracy  $\langle \cos \theta \rangle$ , and the average magnitude of the pheromone gradient,  $\langle |\nabla[P]| \rangle$ , as functions of the inverse screening length,  $1/\lambda$ . We placed 10,000 cells randomly in a three-dimensional cube and calculated the pheromone gradient at the centre. The screening length,  $\lambda$ , was normalized by the mean distance between cells; the average strength of the gradient was normalized by its maximum (obtained for zero screening, with  $\lambda = \infty$ );  $\theta$  is the angle between the direction of the gradient and the direction to the cell nearest the centre. Detection accuracy increases rapidly for  $\lambda \approx 1$ . Minimum accuracy occurs at  $\lambda = \infty$ , which corresponds to an error of  $\theta = 50^\circ$ . Inset, effect of the *bar* protease on the detection of the nearest mating partner. Blue columns show percentage of cells exposed to a pheromone gradient with normalized values of more than 1%. Green columns show the probability that this gradient will point to within  $20^\circ$  of the nearest α-cell. Strain names are arbitrary: *bar-* indicates cells that do not secrete protease; *bar+*, protease-secreting cells with  $1/\lambda = 4$ ; and *bar++*, cells that secrete a higher level of protease, with  $1/\lambda = 10$ .